DTU Library

Angle-dependent Absorption Property of 2D Infinite Periodic Arrangements of Helmholtz Resonators

Agudelo, Diana Maria Garza; Jeong, Cheol-Ho; Andersen, Peter Risby; Cutanda Henriquez, Vicente

Published in:
Forum Acusticum 2020

Publication date:
2020

Document Version
Publisher's PDF, also known as Version of record

ANGLE-DEPENDENT ABSORPTION PROPERTY OF 2D INFINITE PERIODIC ARRANGEMENTS OF HELMHOLTZ RESONATORS

Diana Maria Garza-Agudelo, Cheol-Ho Jeong, Peter Risby Andersen, and Vicente Cutanda Henriquez
Department of Electrical Engineering, Technical University of Denmark, Denmark
dmgag@elektro.dtu.dk

ABSTRACT

In recent years, the potential of sound absorbing metamaterials as an alternative to traditional acoustic absorbers has been demonstrated in several publications. A common way to design these absorbing metamaterials, is through periodic arrangements of resonators. By combining acoustic resonators tuned to different resonance frequencies in each unit cell, the frequency range for which the material achieves high absorption can be extended. Nevertheless, there is limited research on their behavior when they are exposed to waves incident at oblique directions, and this information is highly relevant for a large amount of practical applications; particularly in room acoustics. In this work, the finite element method (FEM) is used, to study the angle-dependent absorption properties of infinitely large 2D surfaces consisting of a periodic arrangement of Helmholtz resonators. It is found that the incidence angle influences not only the magnitude of the (maximum) absorption coefficient, but also the frequencies at which the maximum absorption coefficient is observed, as well as the absorption bandwidth.

1. INTRODUCTION

Within the acoustic metamaterials field, alternative solutions have been proposed to obtain structures that display properties that are not found in traditional elements. Among this cases, elements that can achieve negative refraction or acoustic cloaking, as well as light weight structures with high transmission loss and absorbing materials with a very small thickness to wavelength ratio are some examples [1, 2]. In the design of metamaterials, the particular behaviour of periodic arrangements of elements, is often exploited for sound insulation [3–5], absorption [6–8] and diffusion [9] applications.

More explicitly, for the applications related to sound absorption, periodic arrangements of resonators tuned to different frequencies are used in order to create surfaces that would have a smaller thickness to wavelength ratio, compared to what can be achieved using porous materials; and at the same time, a frequency range of high absorption coefficient values that is broader than what can be achieved using a surface composed of only one a single type of resonator [6–8, 10].

In many practical applications, absorbing materials are exposed to incoming waves from directions which are not normal to the surface; several room acoustic applications among this. Even though the potential of periodic arrangements of resonators as acoustic absorbing materials has been demonstrated in published works, the characterization of their behaviour is typically done in terms of their normal incidence absorption coefficient. As can already be seen in the work by Gao et al. [11], changes in the incidence angle can include both changes in the absorption coefficient value per frequency, as well as the span of the frequency range for which a high performance is achieved. Therefore, there is a need to study the behaviour of this periodic surfaces at oblique incidence. Knowing such oblique incidence absorption properties will enhance the accuracy of computer predictions of room acoustics [12].

This work focuses on the angle-dependent absorption coefficient of surfaces that are composed of periodic arrangements of Helmholtz resonators. The surfaces extend infinitely both in the directions parallel and perpendicular to the slits in the plane of the surface. For this purpose, a 2D numerical study has been conducted on surfaces made of periodic arrangements of 1, 2 and 3 different types of resonators. The surface consisting on a periodic arrangement of a single resonator is included as the baseline example for periodic surfaces. In turn, including the surfaces consisting of a periodic arrangement of a unit cell composed of 2 types of resonators, allows to observe the behaviour of the surfaces when the unit cell starts to be heterogeneous. And, the surfaces consisting of a periodic arrangement of a unit cell composed of 3 types of resonators, shows a generalization of the angle-dependent absorption properties of surfaces composed of several different resonators.

In section 2 of this document, a description of the surfaces used for this study, and the method to estimate their angle-dependent behaviour are described. In sections 3 and 4, the results describing the angle-dependent absorption properties of the three types of sources analyzed are presented. In section 5 a discussion of the results shown is made. And, in section 6, the conclusions that can be drawn from the present study are included.

2. METHOD

2.1 Test cases included in the present study

In the scope of this work, surfaces constituted by a periodic arrangement of 1, 2 and 3 different 2D Helmholtz resonators are studied. For each of this three cases, two parameters are varied independently in order to see their effect on the resonators' performance. This parameters are the separation distance between adjacent resonators (identified as d in Figure 1), which is varied between 3 cm to 9 cm in steps of 2 cm; and the angle of incidence of the incident plane wave with respect to the normal direction, which takes values from 0 to 87^o. As means of illustration, Figure 1 shows an schematic of the unit cell for the surface consisting of 3 different types of resonators. And, table 1 shows the dimensions of the resonators constituting the unit cells of each of the periodic surfaces under study.

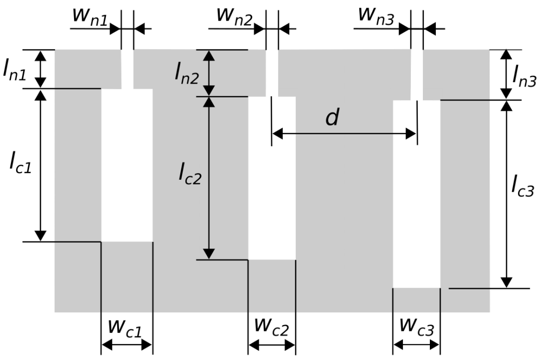

Figure 1: Schematic representation of the unit cell of a surface composed of a periodic arrangement of 3 different 2D Helmholtz resonators.

Surface composed of a periodic arrangement of 1 resonator				
Resonator	w_n [mm]	l_n [mm]	w_c [mm]	l_c [mm]
1	1.6	23	26.8	118.6
Surface composed of a periodic arrangement of 2 resonators				
Resonator	w_n [mm]	l_n [mm]	w_c [mm]	l_c [mm]
1	1.6	23	26.8	118.6
2	1.5	18.7	27.2	90.3
Surface composed of a periodic arrangement of 3 resonators				
Resonator	w_n [mm]	l_n [mm]	w_c [mm]	l_c [mm]
1	1.5	20	27.4	164.4
2	1.6	21.5	25.7	125.8
3	1.5	20	25.6	92.1

Table 1: Dimensions of the elements composing the unit cells of the different types of periodic surfaces under study.

2.2 Modelling method

In order to model the behaviour of the infinite surfaces, a finite element model was implemented and solved using COMSOL Multiphysics. The implementation consists on a 2D model of an air-filled domain, with an incident pressure field comprised of a plane wave at an incidence angle θ ranging from 0 to 87 degrees. At the lower boundary of the domain, one unit cell of the periodic array of resonators is placed. At the upper part of the domain, a perfectly match layer (PML) is placed in order to simulate a semi-infinite space. Furthermore, the surface under study is simulated to be infinite in the horizontal direction by using Floquet periodicity boundary conditions. A sketch of the model is presented in Figure 2, where the unit cell of the surface composed of 3 different resonators is shown.

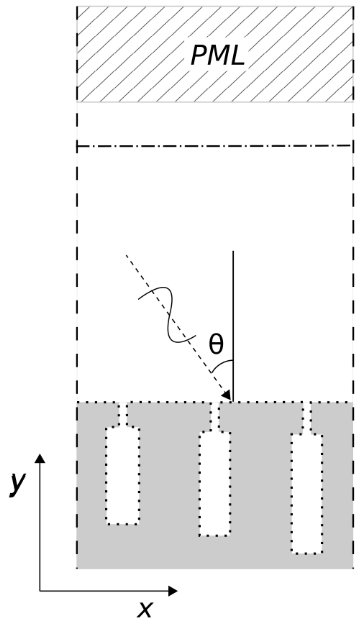

Figure 2: Sketch of the model used for the present study. The case shown corresponds to a surface with 3 resonators tuned to different frequencies. The boundaries identified with the dashed and dotted line, correspond to the boundaries to which a periodic and boundary layer impedance boundary condition was assigned respectively. And, the dotted dashed line identifies the line used for the estimation of the incident and reflected sound power according to Eq. 10. For ease of visualization, the dimensions shown here are not in scale with the dimensions of the model.

Given the plane wave incident pressure field, the problem being solved is described by a homogeneous Helmholtz equation as:

$$\nabla^2 \hat{p_t} + \frac{\omega^2}{c^2} \hat{p_t} = 0 \tag{1}$$

Where ω is the angular frequency, c_0 is the speed of sound in air and $\hat{p_t}$ is the total complex pressure defined as:

$$\hat{p_t} = \hat{p_r} + \hat{p_i} \tag{2}$$

Where p_i is the complex incident pressure field, and p_r is the complex reflected pressure field.

In the same way as the total complex pressure is obtained by adding the incident and reflected complex pressures, the total components of the complex particle velocity can also be obtained by adding up the components of the incident and reflected complex particle velocities. i.e.:

$$\hat{v}_{t,x} = \hat{v}_{r,x} + \hat{v}_{i,x} \tag{3}$$

$$\hat{v}_{t,y} = \hat{v}_{r,y} + \hat{v}_{i,y} \tag{4}$$

Where $\hat{v}_{t,x}$ and $\hat{v}_{t,y}$ are the components of the complex total velocity field, $\hat{v}_{i,x}$ and $\hat{v}_{i,y}$ are the components of the complex incident velocity field, and $\hat{v}_{r,x}$ and $\hat{v}_{r,y}$ are respectively the components of the complex reflected particle velocity field.

Since the problem being modelled corresponds to a surface that is being exposed to a travelling plane wave, the incident pressure field and the components of the incident particle velocity field are defined as:

$$\hat{p_i} = |\hat{p_i}|\mathrm{e}^{i(-k_x x + k_y y)} \tag{5}$$

$$\hat{v}_{i,x} = -\frac{1}{\mathrm{j}\omega\rho}\frac{\partial \hat{p}_i}{\partial x} \tag{6}$$

$$\hat{v}_{i,y} = -\frac{1}{\mathrm{j}\omega\rho}\frac{\partial \hat{p}_i}{\partial y} \tag{7}$$

Where ρ is the air density and k_x and k_y are respectively the components of the wave number in the x-direction and in the y-direction.

By defining the problem in the aforementioned way, using the FEM solution of 1 and Eqs. 2 to 7, the reflected pressure and particle velocity can be obtained. In turn, the intensity of the incident and reflected wave can be obtained as:

$$I_{i,y} = \frac{1}{2}\mathrm{Re}\{\hat{p_i}\hat{v}^*_{i,y}\} \tag{8}$$

$$I_{r,y} = \frac{1}{2}\mathrm{Re}\{\hat{p_r}\hat{v}^*_{r,y}\} \tag{9}$$

Where * identifies the complex conjugate.

And, the absorption coefficient can be estimated as:

$$\alpha = \frac{P_a}{P_i} = 1 - \frac{P_r}{P_i} = 1 - \frac{\int_\mathrm{x} I_{r,y} d\mathrm{x}}{\int_\mathrm{x} I_{i,y} d\mathrm{x}} \tag{10}$$

Where P denotes the acoustic power, and the subscripts a, i, r refer to absorbed, incident and reflected quantities. In turn, the integrals over the x-axis of the intensity, are evaluated numerically over a horizontal line place 2m away from the periodic surface, and 50 cm away from the PML layer (see Figure 2).

Furthermore, in order to account for the viscous and thermal losses taking place inside the resonators, a boundary layer impedance (BLI) boundary condition [13,14] was assigned to the boundaries of the resonators (see Figure 2). For the cases under study here, the use of this boundary condition to estimate losses yield an accurate result because the viscothermal boundary layers do not overlap in the operational frequencies of the resonators.

3. ANGLE DEPENDENT ABSORPTION COEFFICIENT

The present section, will start by presenting the normal incidence acoustic performance of each of the type of surfaces under study for different values of distance between adjacent resonators (d in Figure 1). Then, for a fixed value of d, the angle-dependent absorption coefficient is shown. By comparing the effects of varying d and θ, it is shown that there is a similar effect, and then a description of the behaviour of the periodic surfaces is done in terms of a relationship between d and θ.

Figure 3 shows the absorption coefficient curves at normal incidence as a function of d for each of the surfaces under study. As can be seen, the distance between the resonators, can affect significantly the absorption performance. On the one hand, in the case of the surface made from a single resonator, changing the distance affects mostly the value of the maximum absorption coefficient of the absorber. On the other hand, for the surfaces made from arrays of 2 and 3 types of resonators, a more complex effect can be seen. Namely, it includes a change in the maximum absorption coefficient that the surface can achieve, the regularity of the curve between the peaks of maximum absorption coefficient, and the width of the frequency range for which high absorption coefficient values are seen.

In contrast, in order to visualize the effect of changes in the incidence angle of the plane wave impinging the surfaces, the design with the highest normal incidence absorption coefficients and flatter curve in the region of high performance at normal incidence for each case according the Figure 3, was selected, and evaluated for several incidence angles. In this way, the angle dependency of the absorption properties is studied for the best designs at normal incidence conditions. More explicitly, the values of d selected were 9 cm for the surface consisting of a periodic array of a unit cell composed of a single type of resonator, and 5 cm for the surfaces consisting of a periodic array of a unit cell composed of 2 and 3 types of resonators.

The angle dependent behaviour of the surfaces selected can be seen in Figure 4, where the absorption coefficient for $\theta = 0^o$, 30^o, 45^o, 60^o, and 75^o is shown. When increasing the incidence angle from the normal direction, the changes in the absorption properties have a similar trend to the ones observed on the normal absorption coefficient when decreasing the distance between the adjacent resonators (see Figure 3). Namely, for the surface composed of the unit cell containing a single resonator, as the angle from the normal direction increases, a monotonic decrease of the maximum value of the absorption coefficient is observed. And, for the cases of the surfaces composed of unit cells with more than 1 type of resonator (see Figures 4b and 4c), as the incidence angle increases, the difference in frequency between two contiguous peaks of maximum absorption coefficient starts decreasing. Then, there is a point when adjacent high absorption peaks have merged, and thus, what can be seen is absorption coefficient curves were 1 less absorption peak is present, compared to the curve for normal incidence. Furthermore, the frequencies in which the new absorption coefficient peaks appear, are in the middle of 2 frequencies in which the peaks were originally observed.

In addition to the previous, a complementary observation that can be drawn from Figure 4 is that when the an-

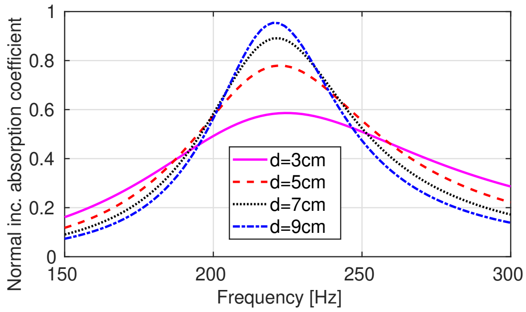

(a) Surfaces with the unit cell composed of a single type of resonator.

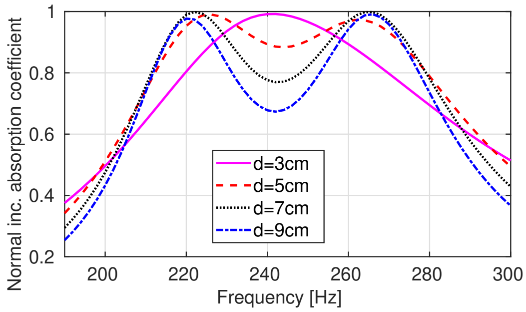

(b) Surfaces with the unit cell composed of 2 different types of resonators.

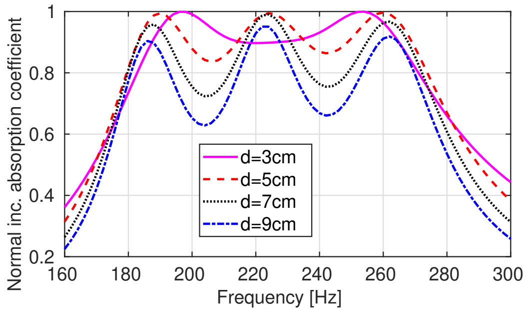

(c) Surfaces with the unit cell composed of 3 different types of resonators.

Figure 3: Normal incidence absorption coefficient of the surfaces consisting of a periodic arrangement of unit cells with 1 (top), 2 (middle) and 3 (bottom) different types of resonators as a function of the distance d between centers of the resonator's entrances.

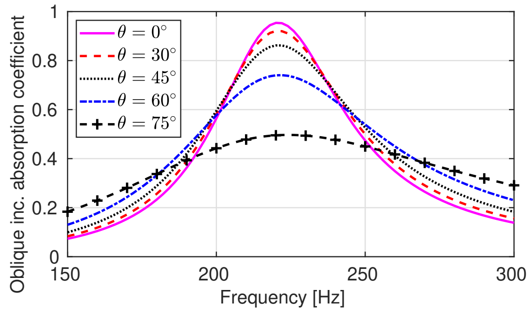

(a) Surface with the unit cell composed of a single resonator with dimensions as shown in Table 1, and a distance between the center of 2 adjacent resonators of 9 cm.

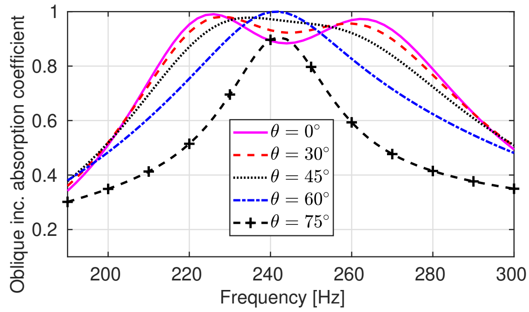

(b) Surface with the unit cell composed of 2 different types of resonators with dimensions as shown in Table 1, and a distance between the center of 2 adjacent resonators of 5 cm.

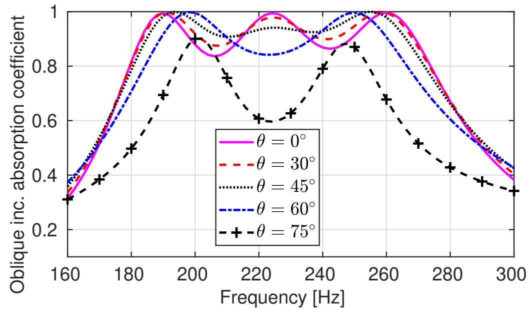

(c) Surface with the unit cell composed of 3 different types of resonators with dimensions as shown in Table 1, and a distance between the center of 2 adjacent resonators of 5 cm.

Figure 4: Angle dependent absorption coefficient of the surfaces consisting of a periodic arrangement of unit cells consisting of 1 (top), 2 (middle) and 3 (bottom) different types of resonators.

gle of incidence becomes large enough, the maximum absorption coefficient that the surface can achieve at any frequency is smaller than the maximum absorption coefficient that can be seen for the case of normal incidence.

In fact, as long as the distance between the resonators is much smaller than the wavelength, as it is the case for the surfaces under study here, the absorption coefficient is dependent on the relationship between the distance separating adjacent resonators and the angle of incidence [15]. More explicitly, the absorption properties are dependent on the parameter $d\cos(\theta)$. Figure 5 evidences this dependency, by comparing, for each of the surfaces under study, the absorption coefficient curves obtained for different values of the parameter $d\cos(\theta)$. It can be seen that for every pair of curves plotted with the same $d\cos(\theta)$ value, the curves coincide. And naturally, it can be then seen that the trend of the changes in the absorption coefficient curves of each of the surfaces under study as the parameter $d\cos(\theta)$ decreases, is comparable to the trend of the changes in the absorption coefficient curves of each of the surfaces under study when the distance between resonators is maintained constant, and the angle of incidence with respect to the normal direction increases (see Figure 4).

4. COMPARISON BETWEEN THE NORMAL AND RANDOM INCIDENCE ABSORPTION COEFFICIENT

As a way to estimate the behaviour of a material in a diffuse environment, the random incidence absorption coefficient can be obtained using Paris formula [16] as shown in

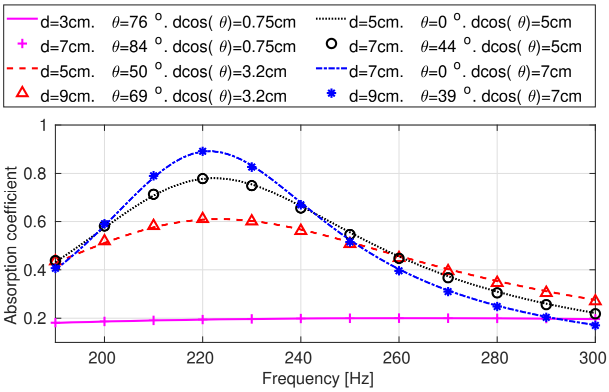

(a) Surface with the unit cell composed of a single resonator.

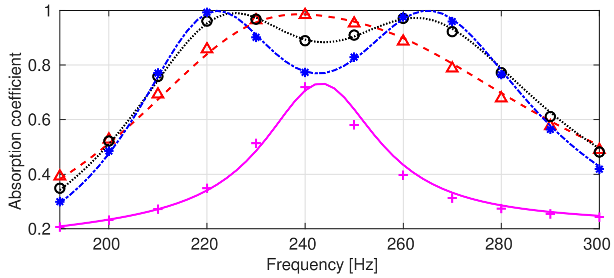

(b) Surface with the unit cell composed of 2 different types of resonators.

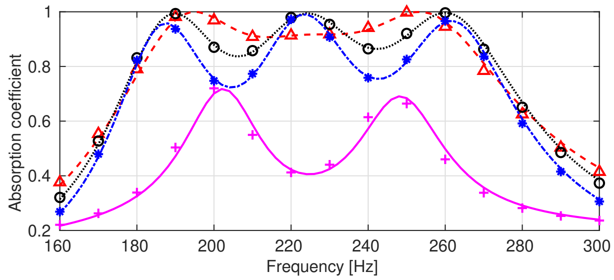

(c) Surface with the unit cell composed of 2 different types of resonators

Figure 5: Absorption coefficient of the surfaces consisting of a periodic arrangement of unit cells with 1 (top), 2 (middle) and 3 (bottom) as a function of the parameter dcos(θ).

Eq. 11. It has been reported that using the normal and random incidence absorption coefficient, room acoustic prediction results vary a lot using both geometrical acoustics and wave-based methods [17, 18]. And although this random coefficient estimate assumes an ideally diffuse condition, which is hard to find in real rooms, it is used here as a reference of the behaviour of the surfaces in e.g. highly reverberant enclosed spaces.

$$\alpha_r = \int_0^{\pi/2} \alpha(\theta) sin(2\theta) d\theta \qquad (11)$$

Figure 6 shows a comparison between the absorption properties at normal and random incidence for: 1) a surface composed of a single type of resonator and d=9 cm (Figure 6a). 2) a surface composed of 2 different types of resonators and d=5 cm (Figure 6b). 3) a surface composed of 3 different types of resonators and d=5cm (Figure 6c).

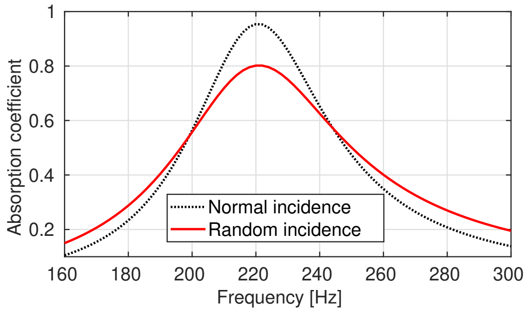

(a) Surface with the unit cell composed of a single resonator with dimensions as shown in Table 1, and a distance between the center of 2 adjacent resonators of 9 cm.

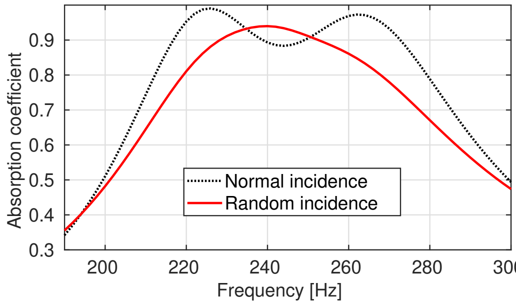

(b) Surface with the unit cell composed of 2 different types of resonators with dimensions as shown in Table 1, and a distance between the center of 2 adjacent resonators of 5 cm.

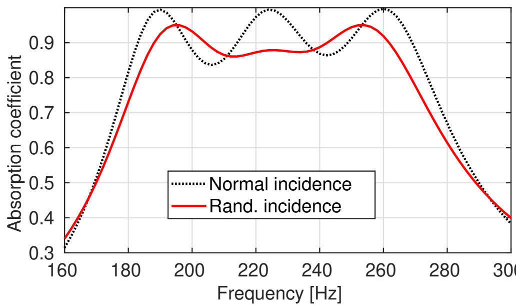

(c) Surface with the unit cell composed of 3 different types of resonators with dimensions as shown in Table 1, and a distance between the center of 2 adjacent resonators of 5 cm.

Figure 6: Comparison between the normal and random incidence absorption coefficient curve of the surfaces consisting of a periodic arrangement of unit cells with 1 (top), 2 (middle) and 3 (bottom) different types of resonators.

Note that the aforementioned selected cases, are the same ones selected to show the absorption properties for selected individual angles (see Figure 4).

As expected, the effects of changes on the incidence angle, as seen in Figure 4, can also be observed when evaluating the performance of the surfaces at random incidence. More explicitly, for the case of the surface with a single type of resonator, the maximum achievable absorption coefficient is lowered; and for the surfaces with more than 1 type of resonators, there is a decrease on both the maximum absorption coefficient that the surface can achieve, and the width of the frequency range of which high acoustic performance.

5. DISCUSSION

The angle-dependent absorption properties of periodic arrangements of 2D Helmholtz resonators consisting on a single or several types of resonators was studied. Given a fixed value of d, for a surface composed of a single type of resonator, the effect of changing the incidence angle is limited to changes in the maximum absorption coefficient that the surface can achieve; but the bell shape of the absorption coefficient curve and the frequency at which the maximum absorption coefficient appears do not change significantly. On the other hand, for surfaces composed of more than one type of resonators, the effect is more complex. It includes changes in the maximum absorption coefficient that the surface can achieve, the frequencies at which the maximum absorption coefficient values are obtained, and the frequency range were a high absorption performance is seen. Thus, when a periodic surface is composed of resonators designed for different operational frequencies, in order to characterize its behaviour at several oblique incidence angles, it is not sufficient to observe the variation of the absorption coefficient at a single frequency (e.g. the frequency for which the maximum normal incidence absorption coefficient happen); instead, a proper characterization of the behaviour should include the evaluation of the performance for all the frequency range of interest, in order to also be able to detect changes in the shape of the absorption coefficient curve.

The absorption properties of the surfaces under study here, where the separation between adjacent resonators is much smaller than the wavelength, are highly dependent on the parameter d$\cos(\theta)$; d being the distance between adjacent resonators, and θ being the angle of incidence from the normal direction to the surface. For large d$\cos(\theta)$ values, there seems to be less interaction between the resonators; this can be stated since in the absorption coefficient curve, the individual peaks related to the resonance frequencies of the individual resonators stand out more, thus, making the absorption coefficient in the intermediate frequencies drop. As the value of d$\cos(\theta)$ decreases, the amount of interaction between the resonators increases, and the peaks in the absorption coefficient curve start approaching each other, also causing the absorption coefficient values in the frequencies between the peaks to drop less. For even lower d$\cos(\theta)$ values, each pair of neighbouring peaks merge, and therefore, in the absorption coefficient curve, there will be one less absorption peak than there are resonators. This behaviour will narrow the bandwidth of high absorption values. Moreover, a further decrease of d$\cos(\theta)$, will cause the global maximum absorption coefficient that can be achieved by the surface to drop. This trend can be seen for both of the cases studied of surfaces consisting of more than one type of resonators, thus it is expected that it is a trend that would also be seen for surfaces consisting of more types of resonators than the ones included in this study.

Finally, when comparing the normal and random incidence absorption coefficients of the surfaces under study here, it can be seen, that the absorption properties of both conditions are not equivalent. Therefore, the importance of characterising the behaviour of these periodic surfaces also for oblique angles is highlighted.

6. CONCLUSIONS

In the present work, the absorption properties of surfaces made from infinite periodic arrangements of 2D Helmholtz resonators at normal and oblique incidence were shown. When the surface is composed of 1 type of resonator, the effect of the incidence direction is limited to changes in the magnitude of the absorption coefficient, but not the overall shape of the absorption coefficient curve. When the surface is obtained through the combination of more than 1 resonator, the effect observed is changes in the magnitude and frequency where the highest absorption coefficient values are achieved, and a narrowing of the frequency range for which the surface can achieve a high performance.

The use of periodic arrangements involving different types of resonant elements, has sparked academic interest recently, because they can extend the bandwidth in which a thin surface efficiently controls acoustic reflections; nevertheless, as can be seen from the present study, care must be taken when evaluating this extension based on the behaviour at normal incidence, if the surface will be exposed to oblique incident waves. Even though the maximum number of resonators included in this study is 3, and in previous scientific works the periodic arrangements can include a larger amount of different elements, the similarities seen on the effects of changing the incident angle for the 2 heterogeneous surfaces in this study, suggests a similar trend can be seen for arrays with larger amount of elements.

When evaluating the extended performance of the periodic surfaces at random incidence, it can be seen that there can be significant differences to the normal incidence behaviour. Therefore, if a particular design of a surface is meant to be used for an application where there will be waves coming from several different directions, e.g. room acoustic applications, the characterization of the absorption performance only for the normal incidence condition, can fail to accurately describe the real performance of the element.

It should be noted that the scope of this investigation is limited to infinite surfaces of Helmholtz resonators with slit openings. The effect of the finiteness of the sample is not considered. And, different effects of the incidence angle might be seen in surfaces in which there is variation along the out of plane diection from the xy-plane (see Figure 2), like e.g. a periodic surface of Helmholtz resonators with circular necks.

7. REFERENCES

[1] G. Ma and P. Sheng, "Acoustic metamaterials: From local resonances to broad horizons," *Science Advances*, vol. 2, no. 2, p. e1501595, 2016.

[2] V. Romero-Garcia and A.-C. Hladky-Hennion, eds.,

Fundamentals and Applications of Acoustic Metamaterials. John Wiley Sons, Ltd, 2019.

[3] Z. Liu, X. Zhang, Y. Mao, Y. Y. Zhu, Z. Yang, C. T. Chan, and P. Sheng, "Locally resonant sonic materials," *Science*, vol. 289, no. 5485, pp. 1734–1736, 2000.

[4] K. Lu, J. H. Wu, D. Guan, N. Gao, and L. Jing, "A lightweight low-frequency sound insulation membrane-type acoustic metamaterial," *Aip Advances*, vol. 6, no. 2, p. 025116, 2016.

[5] J. H. Vazquez Torre, J. Brunskog, and V. Cutanda Henriquez, "An analytical model for broadband sound transmission loss of a finite single leaf wall using a metamaterial," *Journal of the Acoustical Society of America*, vol. 147, no. 3, pp. 1697–1708, 2020.

[6] W. Jeon and H. Ryoo, "Dual-frequency sound-absorbing metasurface based on visco-thermal effects with frequency dependence," *Journal of the Acoustical Society of America*, vol. 144, no. 3, pp. 1763–1763, 2018.

[7] X. Peng, J. Ji, and Y. Jing, "Composite honeycomb metasurface panel for broadband sound absorption," *Journal of the Acoustical Society of America*, vol. 144, no. 4, pp. EL255–EL261, 2018.

[8] C. Zhang and X. Hu, "Three-dimensional single-port labyrinthine acoustic metamaterial: Perfect absorption with large bandwidth and tunability," *Physical Review Applied*, vol. 6, no. 6, p. 064025, 2016.

[9] N. Jiménez, T. J. Cox, V. Romero-García, and J. P. Groby, "Metadiffusers: Deep-subwavelength sound diffusers," *Scientific Reports*, vol. 7, no. 1, p. 5389, 2017.

[10] N. Jiménez, V. Romero-García, V. Pagneux, and J.-P. Groby, "Rainbow-trapping absorbers: Broadband, perfect and asymmetric sound absorption by subwavelength panels for transmission problems," *Scientific Reports*, vol. 7, no. 1, pp. 13595, 13595, 2017.

[11] Y. x. Gao, Y. p. Lin, Y. f. Zhu, B. Liang, J. Yang, J. Yang, and J. c. Cheng, "Broadband thin sound absorber based on hybrid labyrinthine metastructures with optimally designed parameters," *Scientific Reports*, vol. 10, no. 1, p. 10705, 2020.

[12] G. H. Marbjerg, J. Brunskog, C.-H. Jeong, and E. Nilsson, "Development and validation of a combined phased acoustical radiosity and image source model for predicting sound fields in rooms," *Journal of the Acoustical Society of America*, vol. 138, no. 3, pp. 1457–1468, 2015.

[13] M. Nijhof, *Viscothermal wave propagation*. PhD thesis, University of Twente, Netherlands, 12 2010.

[14] M. Berggren, A. Bernland, and D. Noreland, "Acoustic boundary layers as boundary conditions," *Journal of Computational Physics*, vol. 371, pp. 633–650, 2018.

[15] C. Zwikker and C. Kosten, *Sound absorbing materials*. Elsevier Publishing,,, 1949.

[16] E. Paris, "On the coefficient of sound-absorption measured by the reverberation method," *Philosophical Magazine*, vol. 5, no. 29, pp. 489–497, 1928.

[17] F. Pind, C.-H. Jeong, J. S. Hesthaven, A. P. Engsig-Karup, and J. Strømann-Andersen, "Time-domain room acoustic simulations with extended-reacting porous absorbers using the discontinuous galerkin method," *Accepted in Journal of the Acoustical Society of America*, 2020.

[18] C.-H. Jeong, "Absorption and impedance boundary conditions for phased geometrical-acoustics methods," *Acoustical Society of America. Journal*, vol. 132, no. 4, pp. 2347–2358, 2012.